Experimental Evidence of a Zonal Magnetic Field in a Toroidal Plasma

A. Fujisawa,[1] K. Itoh,[1] A. Shimizu,[1] H. Nakano,[1] S. Ohshima,[1] H. Iguchi,[1] K. Matsuoka,[1] S. Okamura,[1] T. Minami,[1] Y. Yoshimura,[1] K. Nagaoka,[1] K. Ida,[1] K. Toi,[1] C. Takahashi,[1] M. Kojima,[1] S. Nishimura,[1] M. Isobe,[1] C. Suzuki,[1] T. Akiyama,[1] Y. Nagashima,[2] S.-I. Itoh,[2] and P. H. Diamond[3]

[1]*National Institute for Fusion Science, Oroshi-cho, Toki-shi 509-52, Japan*
[2]*RIAM, Kyushu University, Kasuga 816-8580, Japan*
[3]*University of California, San Diego, La Jolla, California 92093-0319, USA*

(Received 1 November 2006; published 18 April 2007)

A zonal magnetic field is found in a toroidal plasma. The magnetic field has a symmetric bandlike structure, which is uniform in the toroidal and poloidal directions and varies radially with a finite wavelength of mesoscale, which is analogous to zonal flows. A time-dependent bicoherence analysis reveals that the magnetic field should be generated by the background plasma turbulence. The discovery is classified as a new kind of phenomenon of structured magnetic field generation, giving insight into phenomena such as dipole field generation in rotational planets.

DOI: 10.1103/PhysRevLett.98.165001 PACS numbers: 52.35.Ra, 52.25.Gj, 52.35.Mw, 52.70.Ds

Nowadays, a number of phenomena analogous to geomagnetism are known to occur ubiquitously in nature: e.g., the planetary dynamo, sun spots, the galactic dynamo, etc. A widely accepted hypothesis is that turbulence should be a main player for the phenomena of magnetic field generation [1–3]. Along with accumulating support for this hypothesis from direct nonlinear simulations [4,5], laboratory experiments have made progress in observing the phenomena associated with a dynamo in turbulent materials [6–13]. For instance, the fundamental processes of a dynamo, such as a self-exciting magnetic field [11] and the generation of a magnetic field by turbulent flows [13], have been demonstrated in experiments using turbulent conducting flows of liquid metals.

In toroidal plasma, which aims at realizing *a Sun on the Earth*, strong turbulence sustained by a steep pressure gradient organizes the thermal structure through self-regulating transport. Recently, a structured electric field driven by microscopic turbulence was identified using heavy ion beam probes (HIBPs) in a toroidal plasma named the compact helical system (CHS) [14]. In a magnetically confined plasma, the electric field is equivalent to the perpendicular flows to the confinement magnetic field through $E \times B$ drift. The structured electric field dubbed *zonal flow* or *zonal electric field* [15] has a coaxial symmetry around the magnetic axis, and it fluctuates with a radial wavelength with a constant phase on a magnetic surface. This field is classified as a *mesoscale*, since the scale of the radial wavelength is larger than the characteristic scale of the turbulence but smaller than the system size.

Current theory suggests the possibility that turbulence should generate a zonal magnetic field in addition to a zonal flow [15–18]. Similarly to the zonal flow, the zonal magnetic field fluctuates homogeneously on the magnetic surface and alternates direction as a function of plasma radius. This field therefore remains finite even upon averaging over a magnetic surface to be regarded as a *mean* field. The HIBP has an ability to sense a magnetic field fluctuation simultaneously with an electric field one. Trials to search a zonal field, utilizing the advantage of the diagnostics, have been performed in CHS. In this Letter, we present the discovery of a zonal magnetic field—a new kind of structured magnetic field generated from background turbulence. The present experimental results provide the first clear evidence that turbulence generates a structured magnetic field by directly quantifying their coupling using a bicoherence analysis.

CHS is a device designed to confine a toroidal helical plasma (major radius $R = 1$ m and minor radius $a = 0.2$ m) without a net nominal internal current. The device is equipped with two HIBPs, a unique diagnostic to measure density, electrostatic potential, and vector potential. The HIBPs are located apart from each other by approximately 90 degrees in the toroidal direction. Each of them is capable of measuring three adjacent positions in the plasma. Hence, spatially differential values of measurable quantities can be directly determined by examining the difference between two of three channels. In the previous measurement on zonal flow detection, the electric field fluctuation was directly evaluated from the difference of potentials between two neighboring channels [14].

It has been known for HIBPs, in addition to the electrostatic potential, that a vector potential component can be measured from the beam movement on the detector; particularly in an axisymmetric magnetic configuration, a formula is derived to relate the movement to the toroidal component of the vector potential [19]. In real geometry, the fluctuation of a magnetic field component, or derivative of vector potential, can be directly measured by taking the difference between the beam movements on the detectors from the neighboring ionization points [20].

The target plasma is produced with electron cyclotron resonance heating at ~200 kW, to avoid a large-scale plasma motion caused by magnetohydrodynamic instabilities that interfere with the generation of magnetic fields in the mesoscale range. The plasma parameters in the experiment are the magnetic field strength $B = 0.88$ T, density $n_e \sim 5 \times 10^{12}$ cm^{-3}, electron and ion temperatures $T_e \sim 0.5$ keV and $T_i \sim 0.1$ keV, respectively (i.e., in the collisionless regime), ion Larmor radius $\rho_i \sim 0.1$ cm, time scale of microinstabilities $\omega^*/2\pi R \sim 50$ kHz, with $k_\perp \rho_i = 0.3$ and energy confinement time $\tau_E \sim 2$ ms (or characteristic frequency of global confinement $\tau_E^{-1} \sim 0.1$ kHz), where $k_\perp$ is the wave number and ω^* is the drift frequency defined as $k_\perp T_e/eBL_n$, with L_n being a characteristic length of density gradient. Here the pressure-gradient-driven microinstabilities are associated with electromagnetic field fluctuations [21]. The normalized plasma pressure, β value, is ~0.2%. Collisionless (or electron) and collisional skin depths are estimated as 2.4 and 12 mm at 0.5 kHz, respectively. The magnetic Prandtl number is evaluated as $\mu_0 \nu/\eta \sim 10^2$ using the experimental viscosity of $\nu(\sim\chi) \sim 10$ m^2/s and resistivity of $\eta \sim 10^{-7}$ Ω m, where χ represents the thermal diffusivity evaluated as the global average from the confinement time.

The measurement was done at the radial position of $r_{\rm obs} = 12 \pm 0.5$ cm, where the signal-to-noise ratio is maximal for the HIBP measurement. In this measurement, it is known from a trajectory calculation that the horizontal beam movement reflects the poloidal magnetic field. A spectrum of the magnetic field fluctuation is shown in Fig. 1, with coherence between two toroidal locations. The dashed line is the estimated maximum (or the upper boundary) of contamination due to the electric field fluctuation at the observation point [20,22]. In the low frequency range, the contamination is sufficiently small, while the electric field contamination may be dominant around ~50 kHz and above. The coherence of the frequency lower than 1 kHz is quite high (~0.7), which is an average of ~70 temporal windows from identical shots; a higher coherence value is obtained in an appropriate period of a single shot. This means that the probing beams are coherently swung by the magnetic field at two toroidal

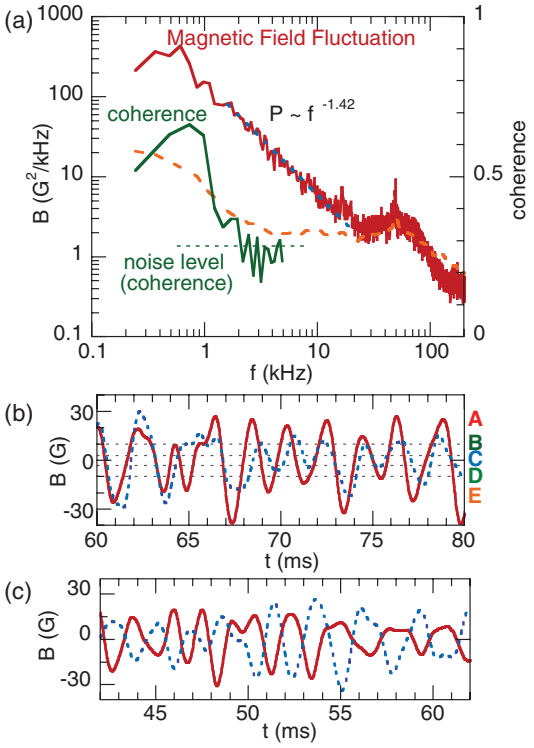

FIG. 1 (color). Magnetic field fluctuation spectrum and existence of the mean field. (a) Power spectrum (poloidal component) and coherence between the magnetic field at two toroidal locations. The fluctuation less than ~1 kHz shows a quite high coherence, which means generation of a global magnetic field of azimuthal symmetry. The spectrum is calculated for the stationary period of ~50 ms for the discharge duration of ~100 ms with a frequency resolution of 0.24 kHz and a Nyquist frequency of 250 kHz. (b) The waveforms of zonal fields at the same radial but different toroidal locations. The positive sign means the direction of vacuum field direction. (c) The other waveforms of zonal fields at the different positions in both the toroidal and radial directions. The difference in radial direction is 1 cm.

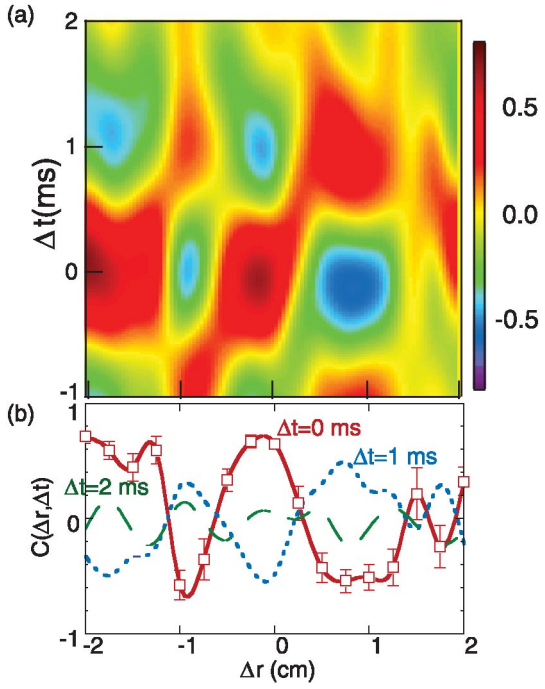

FIG. 2 (color). Radial structure of the zonal field. (a) Correlation function of space and time, $C(\Delta r, \Delta t)$, around the radial position of $r = 12$ cm. (b) Correlation functions with three different time delays;$\Delta t = 0$, 1, and 2 ms. These correlation diagrams show radial structure of zonal field, which has a quasisinusoidal radial structure with a characteristic radial wavelength (~1 cm) in mesoscale. On the other hand, the temporal correlation indicates that the memory of the mesoscale structure fades away with oscillation in ~2 ms.

positions. It is unambiguously demonstrated that a mean magnetic field fluctuation with long-distance correlation does exist.

The magnetic field fluctuations in that frequency range are visualized using a low-pass filter [14]. Figures 1(b) and 1(c) demonstrate two examples of evolution of the magnetic field fluctuation in the frequency range (0.3–1 kHz). The zonal field amplitude is evaluated to be ~30 G at maximum. The accuracy of the absolute magnetic field value is about ±50% owing to uncertainty in the absolute measurement of beam location, although the relative motion of the beam is more precisely measured with an accuracy of ~0.1%. The in-phase movement of two beams on the same magnetic flux surface [Fig. 1(b)] suggests that the fluctuation is symmetric or homogeneous around the magnetic axis under the assumption of poloidal symmetry. In contrast, the other waveforms in antiphase behavior [Fig. 1(c)], when the position is different in radial direction by 1 cm from the other, suggest that the fluctuation should have a finite radial structure.

A constant phase relation between the signals from two different radial positions, as is shown in Figs. 1(b) and 1(c), allows us to estimate the spatiotemporal characteristics of the mean zonal field in the radial direction by calculating the correlation function, defined as $C(\Delta r, \Delta t) = \langle B_{\mathrm{ZMF}}(r,t) B_{\mathrm{ZMF}}(r',t')\rangle / \sqrt{\langle B^2_{\mathrm{ZMF}}(r,t)\rangle \langle B^2_{\mathrm{ZMF}}(r',t')\rangle}$, with $\Delta r = r' - r$ and $\Delta t = t' - t$, where $\langle\,\rangle$ means temporal average, defined as $\langle g(t)\rangle = T^{-1}\int_{t-T/2}^{t+T/2} g(s)ds$, and B_{ZMF} is the filtered signal of the magnetic field. Figure 2(a) shows the cross correlation obtained by altering an observed position r', shot by shot with fixing the other at r (= 12 cm). Figure 2(b) illustrates the spatial structure of 3 times at $\Delta t = 0$, 1, and 2 ms. These correlation diagrams show a quasisinusoidal structure in the radial direction with a characteristic radial wavelength of $\lambda_r \sim 1$ cm, while memory of the structure is lost in ~2 ms. These observations in Figs. 1 and 2 show, therefore, the existence of the mean magnetic field with radially zonal structure symmetric around the magnetic axis. This magnetic field resistively damps away, if there is no driving source, on a time scale of $\tau_R = \mu_0 \eta^{-1} k_r^{-2} \sim 50\ \mu$s. It cannot be sustained by the external circuit through inductive coupling, because the direction changes with radius. It therefore must be sustained by the internal plasma dynamics.

A bicoherence analysis [23] is able to quantify the nonlinear coupling strength between waves. The bicoherence analysis becomes to acquire temporal resolution based on a wavelet instead of traditional Fourier transformation. Here we applied the bicoherence analysis using Gabour's wavelet to prove the existence of the couplings between zonal fields and turbulent waves, which could be intermittent, owing to their disparate scale difference; the temporal scale of turbulence is roughly a hundred times shorter than that of a zonal field in CHS. Actually, the application of the wavelet bicoherence succeeded in extracting intermittent coupling between zonal flow and turbulence [24].

Figure 3 shows some of the results obtained on the bicoherence diagrams and the total bicoherence. The wavelet analysis is done using a conditional average according to the five phases of the zonal field [see Fig. 1(b)]: (A) $B_{\mathrm{ZMF}} > 10$ G, (B) $10 > B_{\mathrm{ZMF}} > 3$ G, (C) $|B_{\mathrm{ZMF}}| < 3$ G, (D) $-3 > B_{\mathrm{ZMF}} > -10$ G, and (E) $B_{\mathrm{ZMF}} < -10$ G. Two bright lines $f_1 + f_2 = \pm 0.5$ kHz in the bicoherence diagrams for phases A and E [Figs. 3(a) and 3(c)] clearly demonstrate that nonlinear couplings between turbulence fluctuation and zonal field increase when the zonal field stays near the maxima and the minima. On the other hand, no significant coupling is seen in phase C [Fig. 3(b)].

In order to quantify this dependence, the total bicoherence β^2 is shown in Fig. 3(d) for all phases. It is obvious that the total bicoherence becomes larger as the zonal field becomes closer to its maximum or minimum (or phases A or E). Figure 3(e) shows explicitly the total bicoherences β^2 at 0.5 and 0.75 kHz as a function of the average of the

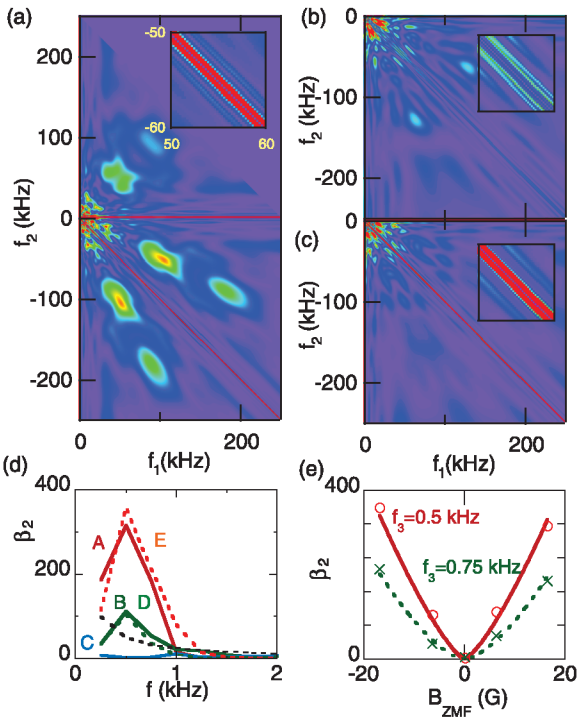

FIG. 3 (color). Coupling of zonal field and turbulence. Bicoherence analysis using Gabour's wavelet to show the existence of a linkage between zonal field and turbulence. Here the analysis adopts the conditional average to take into account the dependence of the coupling on the zonal field phase. Bicoherence diagrams of (a) phase A, (b) phase C, and (c) phase E. The insets are expanded views of a frequency range of $50 < f_1 < 60$ kHz and $-60 < f_2 < -50$ kHz. (d) Total bicoherences in the frequency range below 2 kHz for all five phases. The dashed line shows an estimator giving a rough criterion of convergence. (e) The total bicoherence as a function of the averaged amplitude of the zonal field for the five phases.

zonal field amplitude in each phase, demonstrating that the total bicoherence grows as the absolute value of B_{ZMF} becomes larger. A closer look at elemental bicoherence values reveals that an increase in the couplings of more than $\sim$1 kHz should increase the total bicoherence in phases A and E. In addition, the analysis of the biphase shows that phase is constant along the lines of $f_1 + f_2 = \pm 0.5$ kHz above 1 kHz, suggesting that the modulational instabilities should play an important role in the field generation, as is expected from theories [15,16]. Therefore, wavelet bicoherence analysis verifies the existence of the coupling between zonal field and turbulence and its intermittent behavior associated with the zonal field phase, even if the measured turbulence is a mixture of electrostatic and magnetic fluctuations.

The contamination of electric field fluctuation in the turbulence regime may disturb the absolute quantification of the coupling between the zonal field and the pure magnetic field turbulence. Although the upper boundary of the contamination is comparable to that of the magnetic field fluctuations in the turbulence regime around $\sim$50 kHz (see Fig. 1), the coherence between the local electric field and magnetic field fluctuations is found to be statistically significant but not so high. Consequently, the actual electric field contamination in this frequency regime should not be as large as the level of the upper boundary. The degree of the contamination could be evaluated more precisely in a future analysis by taking into account the detailed fluctuation properties.

Finally, the presented observations verify the existence of zonal magnetic field, as well as zonal flow, generated from the turbulence, probably through modulational instabilities. From the analogy to the zonal flows in Jupiter, future observations might find zonal magnetic field structure in a rotating star. A residual macroscopic field could be expected even in the average over the whole zonal structure, in an inhomogenous background. In addition, the zonal field could serve as a *seed*, leading to global instabilities to cause a macroscopic field or dynamo. Therefore, the discovery could be a step toward general understanding of the dynamo problem, stimulating a question of whether the mesoscopic zonal field can be developed into a macroscopic structure.

We thank Professor O. Motojima for his continuous support and Professor Shibahashi, the University of Tokyo, for his valuable comments. We also thank Mr. K. Miyajima, Ms. S. Itoh, and Mr. R. Akiyama for their CHS operation and Mr. I. Ohtawa at Shonan Giken Co., Mr. A. Shimizu at Shosei Industry, and Mr. S. Wakuta at Sanwa Shoji Co. for their help with HIBP construction. This work is partly supported by the Grant-in-Aids for Specially-Promoted Research (No. 16002005) and Scientific Research (No. 18360447).

[1] H. K. Moffat, *Magnetic Field Generation in Electrically Conducting Fluids* (Cambridge University Press, Cambridge, England, 1978).
[2] A. Yoshizawa, S.-I. Itoh, K. Itoh, *Plasma and Fluid Turbulence* (Institute of Physics, Bristol, 2002).
[3] L. M. Widrow, Rev. Mod. Phys. **74**, 775 (2002).
[4] P. H. Roberts and G. A. Glatzmaier, Rev. Mod. Phys. **72**, 1081 (2000).
[5] J. Li, T. Sato, and A. Kageyama, Science **295**, 1887 (2002).
[6] H. Ji, S. C. Prager, A. F. Almagri, J. S. Sarff, Y. Yagi, Y. Hirano, K. Hattori, and H. Toyama, Phys. Plasmas **3**, 1935 (1996).
[7] D. R. Sisan, N. Mujica, W. A. Tillotson, Y. M. Huang, W. Dorland, A. B. Hassam, T. M. Antonsen, and D. P. Lathrop, Phys. Rev. Lett. **93**, 114502 (2004).
[8] M. D. Nornberg, E. J. Spence, R. D. Kendrick, C. M. Jacobson, and C. B. Forest, Phys. Rev. Lett. **97**, 044503 (2006).
[9] F. Petrelis, M. Bourgoin, L. Marie, J. Burguete, A. Chiffaudel, F. Daviaud, S. Fauve, P. Odier, and J. F. Pinton, Phys. Rev. Lett. **90**, 174501 (2003).
[10] N. L. Peffley, A. B. Cawthorne, and D. P. Lathrop, Phys. Rev. E **61**, 5287 (2000).
[11] A. Gailitis *et al.*, Phys. Rev. Lett. **84**, 4365 (2000).
[12] U. Mueller and R. Stieglitz, Naturwissenschaften **87**, 381 (2000).
[13] R. Monchaux *et al.*, Phys. Rev. Lett. **98**, 044502 (2007).
[14] A. Fujisawa *et al.*, Phys. Rev. Lett. **93**, 165002 (2004).
[15] P. H. Diamond, K. Itoh, S.-I. Itoh, and T. S. Hahm, Plasma Phys. Controlled Fusion **47**, R35 (2005).
[16] I. Gruzinov, A. Das, P. H. Diamond, and A. Smolyakov, Phys. Lett. A **302**, 119 (2002).
[17] L. Chen, Z. Lin, R. B. White, and F. Zonca, Nucl. Fusion **41**, 747 (2001).
[18] P. N. Guzdar, R. G. Kleva, A. Das, and P. K. Kaw, Phys. Rev. Lett. **87**, 015001 (2001).
[19] T. P. Crowley, IEEE Trans. Plasma Sci. **22**, 291 (1994).
[20] A. Fujisawa, A. Shimizu, H. Nakano, and S. Ohshima, Plasma Phys. Controlled Fusion (to be published).
[21] B. B. Kadomtsev, *Plasma Turbulence* (Academic, New York, 1966).
[22] Electric field fluctuation can cause beam energy fluctuation, which should swing the probing beam orbit. This effect should result in the contamination of the electric field fluctuation into the measurement of magnetic field fluctuation.
[23] Y. C. Kim and E. J. Powers, IEEE Trans. Plasma Sci. **PS-7**, 120 (1979).
[24] A. Fujisawa *et al.*, Plasma Phys. Controlled Fusion (to be published).